Published in final edited form as:
Drug Alcohol Depend. 2012 August 1; 124(3): 223–228. doi:10.1016/j.drugalcdep.2012.01.013.

Opioid receptor expression in human brain and peripheral tissues using absolute quantitative real-time RT-PCR

Jinsong Peng[a,#], **Sraboni Sarkar**[a], and **Sulie L. Chang**[a,b,*]

[a]Institute of Neuroimmune Pharmacology, Seton Hall University, 400 South Orange Avenue, South Orange, NJ 07079, USA

[b]Department of Biological Sciences, Seton Hall University, 400 South Orange Avenue, South Orange, NJ 07079, USA

Abstract

Background—The actions of endogenous opioid peptides are mediated by 3 main classes of opioid receptors; mu (MOR), kappa (KOR), and delta (DOR).

Methods—We developed an absolute quantitative real-time reverse transcriptase PCR (AQ-rt-RT-PCR) assay to quantify MOR, DOR, and KOR mRNA in 22 human tissues.

Results—MOR mRNA was greatly enriched ($12 – 20 \times 10^6$ copies/μg) in the cerebellum, nucleus accumbens, and caudate nucleus; moderate (6×10^6 copies/μg) in the dorsal root ganglion, spinal cord, and adrenal gland; low (2×10^4 copies/μg) in the pancreas and small intestine; and absent in the lung, spleen, kidney, heart, skeletal muscle, liver, and thymus. High levels ($>8.8 \times 10^6$ copies/μg) of DOR mRNA were expressed in the brain and dorsal root ganglion; moderate (1.5×10^6 copies/μg) in the adrenal gland and pancreas; low ($2 \times 10^4 – 6.5 \times 10^5$ copies/μg in the cerebellum, spinal cord, small intestine, skeletal muscle, thymus, lung, and kidney); and very low (3.8×10^3 copies/μg) in the heart. DOR mRNA was not detected in the spleen or liver. KOR mRNA was moderate (1×10^6 copies/μg) in brain regions and dorsal root ganglion, but low ($1.6 – 7 \times 10^5$ copies/μg) in the cerebellum, temporal lobe and all other peripheral tissues.

Conclusions—Our data demonstrate that the AQ-rt-RT-PCR is a highly reproducible and precise method to study the expression of opioid receptors in various tissues and under different disease conditions.

*Correspondence to: Sulie L. Chang, 400 South Orange Avenue, South Orange, NJ 07079 USA. Tel: (973) 761-9456; FAX: (973) 275-2489; sulie.chang@shu.edu.
#Jingson Peng's current address is: Wuhan Centers For Disease Prevention and Control, 24#, Jiang-han-bei-lu, Jiang'an District, Wuhan, Hubei 430015, PRChina

Contributors

Jinsong Peng and Sulie L. Chang were involved in the design of the experiments; Jinsong Peng performed the experiments and the data analysis. Jinsong Peng, Sraboni Sarkar, Erik Langsdorf, and Sulie L. Chang were involved in the final preparation of the manuscript and have approved the final version.

Conflict of Interest

No conflict declared.

Keywords

Opioid receptors; quantitative RT-PCR; brain; peripheral tissues

1. Introduction

Since their discovery in 1973 (Pert and Snyder, 1973; Simon et al., 1973; Terenius, 1973), the opioid receptors (OR) have been the focus of intense research with the goal of elucidating their roles in neurotransmission and addiction. To date, three sub-types of OR have been identified – mu (MOR), kappa (KOR), and delta (DOR) [Lord et al., 1977; Martin et al., 1976]. These three types of OR, which belong to the G-protein coupled receptor family, appear to differ primarily in their affinity for various opioid ligands as well as their cellular distribution.

Historically, it was believed that the anti-nociceptive effects of opioids occurred via their actions within the central nervous system (CNS) [Millan, 1986]. However, it has now been shown that opioid-induced anti-nociception can also be initiated by activation of OR outside the CNS (Stein, 1993; Tegeder et al., 2003). For example, opioid compounds affect various aspects of the immune system, including antibody production, T cell responses, NK cell activity, as well as macrophages and granulocyte chemotaxis and activity (Alicea et al., 1998; Rouveix, 1992; Sharp et al., 2000; Sibinga and Goldstein, 1988).

To better understand the roles of the three types of OR in neurotransmission and addiction, it is important to determine the precise expression pattern of the MOR, DOR, and KOR in human brain and peripheral tissues. The expression of these receptors in humans and rats (Mansour et al., 1995) has previously been analyzed using Northern blotting or *in situ* hybridization, and the results using those two methods revealed spatial and temporal expression patterns, which were interpreted as implying important functional differences. However, those methods were not suitable for absolute quantitation of mRNA copy numbers (Tichopad et al., 2003).

In this study, we used absolute quantitative real-time RT-PCR (AQ-rt-RT-PCR), a remarkably sensitive technique for determining mRNA expression (Bouma et al., 2004; Schmittgen, 2001; Tichopad et al., 2003), to identify more specific and precise distribution pattern for the MOR, DOR, and KOR in human brain and peripheral tissues. The use of AQ-rt-RT-PCR to quantify MOR, KOR, and DOR mRNA copies in central and peripheral tissues has a distinct advantage over Northern blotting, *in situ* hybridization, and relative real-time PCR. AQ-rt-RT-PCR enables the investigator to observe physiologically important differences at the mRNA copy level, not simply a relative comparison of fold differences. Unlike fold difference that has to be compared each time to a control sample, copy number provides easy comparison across samples since it a quantitative value, rather than a relative number. Aq-rt-RT-PCR assigns a ‘copy number’ value to gene expression similar to other physiological parameters, which would not only reflect the physiological condition of the particular tissue but can also be easily compared across different samples. One can also examine the distribution of a particular mRNA in a disease state across different tissues. Copy number assessment can provide additional insight into potential biologically relevant outcomes relating to receptor function that could otherwise be missed by relative comparisons. For example, both 1 to 10 copies and10 to 100 copies indicate a 10-fold increase in mRNA; yet the latter means that there was an absolute increase of an additional 90 copies compared to just 9 copies. Therefore, AQ-rt-RT-PCR provides an absolute count of receptor mRNA, and at the same time, allows relative comparisons with quantitation. The sample results are not only normalized to an internal standard (GAPDH), but also to a wide-

range OR standard curve, which provides a precise measurement of gene expression. This enables easy comparison of the OR levels in different tissues since all the samples are normalized to identical standards.

We have further developed and used aq-rt-RT-PCR for other genes of interest. This quantitative assessment of mRNA level thus proves to be an efficient molecular tool in the field of gene expression.

2. Materials and Method

2.1 Tissue acquisition

Total human RNA from the CNS and peripheral tissues was obtained from Clontech (Mountain View, CA). The total RNA was extracted and pooled from males and females (ages: 18 – 57yrs). All of the individuals were disease free and died from sudden natural causes. RNA integrity was confirmed by agarose gel electrophoresis, and the purity was estimated by the OD_{260}/OD_{280} absorbance ratio (1.9 – 2.1). Measurement of RNA concentration was conducted at OD_{260} on a Nano Drop ND-1000 spectrophotometer (Thermo Scientific, Waltham, MA). cDNA was synthesized using Moloney murine leukemia virus (M-MLV) reverse transcriptase (Invitrogen, Carlsbad, CA) and random hexamer primers. Each 20 μl reverse transcription reaction mixture containing 1 μg of human tissue total RNA, 0.1 μl of 3 μg/μl random hexamer primers, 4 μl of PCR buffer (5X), 2 μl of 2.5 μM deoxyribonucleoside 5-triphosphates, and RNase-free water. Reverse transcription was allowed to occur at 37°C for 1 h after adding 200 U of the MMLV-RT. The reaction mixture was then heated to 67°C for 10 min in order to inactivate the MMLV-RT. The cDNA solution was then stored at −20°C until use. Non-reactivity of the primers and probe with contaminating genomic DNA was tested by the inclusion of controls that omitted the reverse transcriptase enzyme from the cDNA synthesis reaction (no RT controls). All cDNA synthesis was performed in triplicate.

2.2 Real-time PCR primers and probes

We used previously published primers and probes for the MOR, DOR, and KOR (Salemi et al., 2005). All oligonucleotides were custom synthesized by Integrated DNA Technologies (Coralville, IA). The sequences are presented in Table 1. The primers and probes were re-suspended in TE buffer and stored at −30°C until used.

2.3 Preparation of the MOR, DOR, and KOR RNA standards

RT-PCR was used to generate MOR, DOR, and KOR cDNA from NMB human neuroblastoma cells, previously shown to have specific opiate binding sites (Ard et al., 1985). Total RNA was reverse transcribed into cDNA using the random primer [p(dN)6] (Roche Molecular Biochemicals, Indianapolis, IN). The cDNA was amplified by PCR with the appropriate primer pair for MOR, DOR, or KOR. The PCR amplified products were separated on a 3% agarose gel, and purified with the Wizard PCR Preps DNA Purification System (Promega, Madison, WI). The purified MOR, DOR, and KOR cDNA was cloned into a pCR II TOPO vector using the Eukaryotic TOPO TA Cloning Kit (Invitrogen Corp., San Diego, CA). The cloned plasmids containing cDNA of the MOR, DOR, and KOR were then purified with the Pure Link Quick Plasmid Miniprep (Invitrogen, Carlsbad, CA). The presence and orientation of the cDNA inserts of the MOR, DOR, and KOR were determined by restriction enzyme EcoRI digestion and DNA sequencing. The purified plasmids containing MOR, DOR, and KOR cDNA were linearized by restriction enzyme EcoRV digestion, and purified by phenol-chloroform extraction and alcohol precipitation. These cloned plasmids containing MOR, DOR, and KOR cDNA were then transcribed into specific RNA using the MEGAscript kit (Ambion, Austin, TX). MOR, DOR, and KOR

RNA were purified with phenol-chloroform extraction and alcohol precipitation. The concentration and quantity of purified RNA was determined by spectrophotometry, and RNA copy numbers were calculated based on the total MOR, DOR, and KOR RNA transcript products and their molecular weights. Ten-fold serial dilutions of known amounts of MOR, DOR, and KOR transcripts were used as standards.

2.4 Preparation of GAPDH RNA standard for real-time RT-PCR

MOR, DOR, and KOR mRNA levels in the samples were normalized to GAPDH by real-time RT-PCR (Hirst et al., 2003; Lai et al., 2003). A known amount of total RNA standard, extracted from pooled human spleen, was serially diluted (ranging from 8 ng to 1000 ng) and used as the standard to quantify GAPDH mRNA levels in the human tissue samples by real-time RT-PCR. The human tissue samples were amplified in the same plate with the standard under identical conditions. The quantity (ng) of total RNA in the samples was automatically calculated by the ABI Prism 7000 Sequence Detection System (Applied Biosystems, Carlsbad, CA), based on the data obtained from the total RNA standard curve. All amplification reactions were performed in duplicate, and an average RNA quantity (ng) of the duplicate was used to normalize MOR, DOR, and KOR mRNA levels in the human tissue samples. In order to normalize the MOR, DOR, and KOR mRNA levels, the MOR, DOR, and KOR copy numbers in human tissue samples were divided by the total GAPDH RNA in the same sample, as determined by real-time RT-PCR, then converted to the copy number of MOR, DOR, and KOR mRNA/μg of total RNA, and expressed as the mean copy number of mRNA/μg of total RNA.

2.5 Real-time PCR assay

The ABI Prism 7000 Sequence Detection System (ABI 7000 SDS) was used for real-time PCR analysis. Thermal cycling conditions were designed as follows: initial denaturation at 95°C for 10 min, followed by 40 to 45 cycles at 95°C for 15 s, and 60°C for 1 min. For each PCR, 1 μl of cDNA template was added to 24 μl of PCR master mixture containing 12.5 μl of Taqman Universal PCR Master Mix (Applied Biosystems, Carlsbad, CA), 0.5 μl of 20 μM primer and probe, and 10 μl of PCR-grade water. To generate the MOR, DOR, and KOR RNA standard curves in human tissue, known amounts of the MOR, DOR, and KOR RNA standards were serially diluted10-fold, then amplified in the same plate under identical conditions. The quantity of MOR, DOR, and KOR mRNA in the samples was automatically calculated by the ABI 7000 SDS based on the data obtained from the standard curve. All amplification reactions were performed in duplicate for each human tissue, and the data are shown as the mean ± S.E.M. from triplicate reverse transcription reactions.

3. Results

3.1 Determination of real-time RT-PCR linearity, efficiency, and precision

Amplification of the MOR, DOR, KOR, and GAPDH RNA standards showed linearity over a 4 – 6 order range of magnitude, and the correlation coefficients (R^2) were 0.9993, 0.9988, 0.9986, and 0.9955, respectively (Fig. 1).

To determine the PCR efficiency, the slope of the standard curve was assessed for each primer/probe set. In all cases, the slope of the standard curve was close to −3.3, indicating maximum PCR amplification efficiency.

To determine the variation of repetitive measurements of the real-time PCR performed separately two to three days apart, 10-fold serial dilutions of the MOR, DOR, KOR, and GAPDH RNA standards were amplified by real-time RT-PCR in 4 – 5 separate experiments. The coefficients of variation (CV) of the inter-assay threshold cycle (CT) values for the

KOR, MOR, DOR, and GAPDH ranged from 1.32% – 1.87%, 1.31% – 2.31%, 0.35% – 2.90%, and 1.68% – 2.06%, respectively (Table 2).

The ct values of the assays from separate days and the variations between dilutions were similar. The intra-assay ct values for KOR, as measured in four separate experiments, are shown in Table 3. The results were similar for MOR, DOR, and GAPDH (not shown). These data demonstrate the high accuracy and reproducibility of the method and the reproducibility of the assay.

In addition, the intra-assay CVs for the MOR, DOR, KOR, and GAPDH were evaluated using human tissue total RNA as templates. There were six replicates per sample in each assay. The intra-assay CV values for KOR, MOR, DOR, and GAPDH ranged from 0.60% – 1.89%, 0.08% – 2.77%, 0.47% – 1.46%, and 0.18% – 1.67%, respectively (Table 2).

The intra-assay ct values for KOR in the different human tissue samples using 6 replicates were similar (Table 4). Similar results were also obtained for MOR, DOR, and GAPDH (not shown). There was no genomic DNA contamination in the samples as demonstrated by a lack of amplification for MOR, DOR, or KOR cDNA in the non-RT controls.

3.2 Human tissue localization

The expression levels of the MOR, DOR, and KOR in the CNS and peripheral tissues are shown as copies/μg of RNA in Table 5. MOR mRNA expression was high ($12 – 20 \times 10^6$ copies/μg) in the cerebellum, nucleus accumbens, and caudate nucleus of the brain, and was moderate ($2 – 8 \times 10^6$copies/μg) in the putamen, cerebral cortex, temporal lobe, hippocampus, substantia nigra and spinal cord. In peripheral tissues, a moderate level ($2 – 6 \times 10^6$ copies/μg) of MOR mRNA was detected in the dorsal root ganglion and adrenal gland. However, MOR mRNA expression was lowest (~2×10^4 copies/μg) in the pancreas and small intestine, and clearly absent in the lung, spleen, kidney, heart, skeletal muscle, liver, and thymus.

DOR mRNA expression was high in most of the CNS areas examined (>15×10^6 copies/μg), with the exception of the spinal cord (6.27×10^6 copies/μg), substantia nigra (1.5×10^6 copies/μg), and cerebellum (2.7×10^5 copies/μg), in which the DOR mRNA levels were moderate to low. In the peripheral tissues, DOR mRNA expression was highest in the dorsal root ganglion (8.8×10^6 copies/μg), moderate ($1.5 – 2 \times 10^6$ copies/μg) in the adrenal gland and pancreas, low ($2 \times 10^4 – 6.5 \times 10^5$copies/μg) in the small intestine, skeletal muscle, thymus, lung, and kidney, and very low in the heart (3.8×10^3 copies/μg). DOR mRNA was not detected in the spleen or liver.

KOR mRNA expression was detected in all the tissues that were examined in this study. KOR mRNA levels were moderate ($1 – 4x\ 10^6$ copies/μg) in most areas of the CNS, and low ($1.5 – 7 \times 10^5$ copies/μg) in the cerebellum, temporal lobe, and spinal cord. A moderate level of KOR mRNA (1.2×10^6 copies/μg) was detected in the dorsal root ganglion, with only low levels (<1.6×10^5 copies/μg) seen in all the other peripheral tissues examined.

4. Discussion

In this study, we have successfully utilized the absolute quantitative real-time RT-PCR (AQ-rt-RT-PCR) assay to quantify MOR, DOR, and KOR mRNA levels in human tissues. This assay uses both specific primers and probes to amplify MOR, DOR, and KOR mRNA. Our data show that, AQ-rt-RT-PCR is a highly sensitive assay with a wide detection range and excellent reproducibility (Tables 2,3 and 4).

With this absolute quantification assay, we could calculate absolute copy numbers of respective opioid receptor mRNA and establish a particular receptor profile in each of the tissues examined. Not only is it possible to characterize expression in different tissues, but this method also enables easy comparison among various tissues. In addition, AQ-rt-RT-PCR provides highly accurate and reproducible data as reflected by the inter- and intra-assay coefficient of variation.

More importantly, we demonstrated that opioid receptors are widely and differentially distributed throughout the CNS, similar to those described previously using other techniques, such as *in situ* hybridization, Northern blotting, RT-PCR, and receptor autoradiography (Mansour et al., 1995; Mansour et al., 1988). The benefit of using AQ-rt-RT-PCR is the quantitative result; more precisely, a number which can be used to evaluate tissue information in terms of gene expression as well as comparison with other tissues or with similar tissues under different treatment conditions.

Using our novel technique, we found that the MOR, in particular, is widely distributed throughout the forebrain, midbrain, and hindbrain, with greatest expression apparent in the cerebellum, nucleus accumbens, and caudate nucleus. This distribution of the MOR is consistent with its suggested role in pain perception as well as sensorimotor integration. The DOR is highly expressed in the cerebral cortex, putamen, nucleus accumbens, caudate nucleus, temporal lobe, and hippocampus. This distribution corresponds with the suggested involvement of the DOR in motor as well as cognitive functioning. Conversely, the KOR is expressed in moderate amounts in many brain areas, with greatest expression in the putamen, nucleus accumbens, and caudate nucleus. The KOR has been implicated in feeding, pain perception, and neuroendocrine function.

OR receptor synthesis occurs in the dorsal root ganglion (DRG) and is axonally transported to the central and peripheral nerves. We detected moderate MOR, DOR, and KOR expression in the DRG. In the spinal cord, opioid's actions on ascending and descending pain pathways results in analgesia (Mansour et al., 1988; Pan et al., 2004; Vaughan et al., 1997). In the present study, MOR, DOR, and KOR expression was found in the ascending pathways of the spinal cord. Stress can also trigger opioid mediated analgesia in the CNS as well as activating the hypothalamic-pituitary-adrenal axis [HPA] (Yamada and Nabeshima, 1995). Thus, it is possible that the stress-activated HPA axis can stimulate the endogenous opioid systems in the CNS (Kapitzke, Vetter and Cabot, 2005). All three classes of OR are expressed in the rat adrenal gland (Wittert et al., 1996), and we detected these three OR in the human adrenal gland as well, suggesting a paracrine or autocrine role for opioid peptides in adrenal function.

Expression of OR in the peripheral nervous system contributes to anti-nociception as reported in numerous clinical and animal studies (Bagnol et al., 1997; Bigliardi-Qi et al., 2004; Fickel et al., 1997; Holzer, 2004; Salemi et al., 2005; Sevcik et al., 2006). Kapitzke et al. (2005) reported that visceral pain in peripheral organs, such as the digestive system, is modulated through the MOR and KOR. In our study, the MOR, DOR, and KOR were expressed in the pancreas and small intestine.

We found DOR and KOR expression in the human heart, which is consistent with what is seen in the rat heart (Wittert, et al., 1996). The finding of DOR and KOR, but not MOR, receptors in the rat and human heart could, in part, suggest a paracrine role for the enkephalins and dynorphins produced locally within cardiac tissue. However, there could be ample spare OR present that are also detected (Chavkin and Goldstein, 1984).

We detected the DOR and KOR in the lung and kidney, and only the KOR in the liver. MOR expression, however, was not detected in the lung, kidney, or liver. Our findings

contradict previous reports that found all three receptor classes in the rat kidney, lung, and liver (Cabot et al., 1994; LeVier et al., 1995; Sato, Terasaki, and Tsuji, 1990; Singhal et al., 1994; Wittert et al., 1996).

The MOR, DOR, and KOR are also expressed on various immune cells, including lymphocytes and macrophages (Bidlack, 2000). We examined OR expression in two immune system organs – the spleen and thymus. We detected DOR and KOR expression in the thymus; however, only KOR expression was seen in the spleen. Levier (1995), however, observed that MOR agonists suppress phagocytosis by splenic macrophages in mice, and Wittert (1996) reported both MOR and DOR expression in the spleen.

The differences that are observed in MOR expression in some tissues in comparison to previous reports could be, in part, due the processing and handling of post-mortem human tissue. Certain genes from post-mortem samples might require extra procurement enhancements (Cummings et al., 2001). MOR expression is probably more sensitive to tissue handling and RNA isolation as compared to KOR and DOR.

In summary, our study is the first to present absolute quantitative measurement of MOR, DOR, and KOR mRNA in human tissues – CNS and periphery. The broad distribution of OR mRNA expression in the peripheral tissues of the body suggests that opioid peptides may play a role in physiological regulation at the peripheral level as well as serve an important function in neural regulation at the CNS level. Our novel approach using AQ-rt-RT-PCR is highly advantageous in quantifying expression of these OR in various tissues, thus enabling tissue characterization and easy comparison. AQ-rt-RT-PCR can also be used in comparing and characterizing tissues undergoing different treatment protocols as well as in pathological conditions. Therefore, this novel technique of absolute quantitation that we have established is a precise and effective tool to use in future studies to characterize the expression of OR in different tissues and conditions. Furthermore, this technique can be applied to measure, quantify and compare expression of other genes of interest and thus can potentially develop into an efficient and useful molecular biology tool.

Acknowledgments

The authors thank Eric J. LeTellier for his assistance with the references for the manuscript, and Drs. Xin Mao and Erik Langsdorf for their helpful critiques of the manuscript during its preparation.

Role of Funding Source

Funding for this study was provided, in part, by the National Institutes of Health (NIH)/National Institute on Drug Abuse (NIDA) grants, R01 DA007058 and K02 DA016149 to SLC; the NIH/NIDA had no further role in the study design, in the collection, analysis, and interpretation of data, in the writing of the report, or in the decision to submit the paper for publication.

References

Alicea C, Belkowski SM, Sliker JK, Zhu J, Liu-Chen LY, Eisenstein TK, Adler MW, Rogers TJ. Characterization of kappa-opioid receptor transcripts expressed by T cells and macrophages. J Neuroimmunol. 1998; 91:55–62. [PubMed: 9846819]

Bagnol D, Mansour A, Akil H, Watson SJ. Cellular localization and distribution of the cloned mu and kappa opioid receptors in rat gastrointestinal tract. Neuroscience. 1997; 81:579–591. [PubMed: 9300443]

Bidlack JM. Detection and function of opioid receptors on cells from the immune system. Clin Diagn Lab Immunol. 2000; 7:719–723. [PubMed: 10973443]

Bigliardi-Qi M, Sumanovski LT, Buchner S, Rufli T, Bigliardi PL. Mu-opiate receptor and Beta-endorphin expression in nerve endings and keratinocytes in human skin. Dermatology. 2004; 209:183–189. [PubMed: 15459530]

Bouma GJ, Hart GT, Washburn LL, Recknagel AK, Eicher EM. Using real time RT-PCR analysis to determine multiple gene expression patterns during XX and XY mouse fetal gonad development. Gene Expr Patterns. 2004; 5:141–149. [PubMed: 15533830]

Cabot PJ, Dodd PR, Cramond T, Smith MT. Characterization of non-conventional opioid binding sites in rat and human lung. Eur J Pharmacol. 1994; 268:247–255. [PubMed: 7957646]

Chavkin C, Goldstein A. Opioid receptor reserve in normal and morphine-tolerant guinea pig ileum myenteric plexus. Proc Natl Acad Sci USA. 1984; 81:7253–7257. [PubMed: 6095280]

Cummings TJ, Strum JC, Yoon LW, Szymanski MH, Hulette CM. Recovery and expression of messenger RNA from postmortem human brain tissue. Mod Pathol. 2001; 14:1157–1161. [PubMed: 11706078]

Fickel J, Bagnol D, Watson SJ, Akil H. Opioid receptor expression in the rat gastrointestinal tract: a quantitative study with comparison to the brain. Brain Res Mol Brain Res. 1997; 46:1–8. [PubMed: 9191072]

Hirst WD, Abrahamsen B, Blaney FE, Calver AR, Aloj L, Price GW, Medhurst AD. Differences in the central nervous system distribution and pharmacology of the mouse 5-hydroxytryptamine-6 receptor compared with rat and human receptors investigated by radioligand binding, site-directed mutagenesis, and molecular modeling. Mol Pharmacol. 2003; 64:1295–1308. [PubMed: 14645659]

Holzer P. Opioids and opioid receptors in the enteric nervous system: from a problem in opioid analgesia to a possible new prokinetic therapy in humans. Neurosci Lett. 2004; 361:192–195. [PubMed: 15135926]

Kapitzke D, Vetter I, Cabot PJ. Endogenous opioid analgesia in peripheral tissues and the clinical implications for pain control. Ther Clin Risk Manag. 2005; 1:279–297. [PubMed: 18360571]

Lai JP, Yang JH, Douglas SD, Wang X, Riedel E, Ho WZ. Quantification of CCR5 mRNA in human lymphocytes and macrophages by real-time reverse transcriptase PCR assay. Clin Diagn Lab Immunol. 2003; 10:1123–1128. [PubMed: 14607877]

LeVier DG, Brown RD, Musgrove DL, Butterworth LF, McCay JA, White KL Jr, Fuchs BA, Harris LS, Munson AE. The effect of methadone on the immune status of B6C3F1 mice. Fundam Appl Toxicol. 1995; 24:275–284. [PubMed: 7737438]

Lord JA, Waterfield AA, Hughes J, Kosterlitz HW. Endogenous opioid peptides: multiple agonists and receptors. Nature. 1977; 267:495–499. [PubMed: 195217]

Mansour A, Fox CA, Akil H, Watson SJ. Opioid-receptor mRNA expression in the rat CNS: anatomical and functional implications. Trends Neurosci. 1995; 18:22–29. [PubMed: 7535487]

Mansour A, Khachaturian H, Lewis ME, Akil H, Watson SJ. Anatomy of CNS opioid receptors. Trends Neurosci. 1988; 11:308–314. [PubMed: 2465635]

Martin WR, Eades CG, Thompson JA, Huppler RE, Gilbert PE. The effects of morphine- and nalorphine- like drugs in the nondependent and morphine-dependent chronic spinal dog. J Pharmacol Exp Ther. 1976; 197:517–532. [PubMed: 945347]

Millan MJ. Multiple opioid systems and pain. Pain. 1986; 27:303–347. [PubMed: 3027643]

Pan YZ, Li DP, Chen SR, Pan HL. Activation of mu-opioid receptors excites a population of locus coeruleus-spinal neurons through presynaptic disinhibition. Brain Res. 2004; 997:67–78. [PubMed: 14715151]

Pert CB, Snyder SH. Opiate receptor: demonstration in nervous tissue. Science. 1973; 179:1011–1014. [PubMed: 4687585]

Rouveix B. Opiates and immune function. Consequences on infectious diseases with special reference to AIDS. Therapie. 1992; 47:503–512. [PubMed: 1301643]

Salemi S, Aeschlimann A, Reisch N, Jungel A, Gay RE, Heppner FL, Michel BA, Gay S, Sprott H. Detection of kappa and delta opioid receptors in skin--outside the nervous system. Biochem Biophys Res Commun. 2005; 338:1012–1017. [PubMed: 16263089]

Sato H, Terasaki T, Tsuji A. Specific binding and clearance of [3H]dynorphin (1–13) in the perfused rat lung: an application of the multiple-indicator dilution method. J Pharm Pharmacol. 1990; 42:879–882. [PubMed: 1983155]

Schmittgen TD. Real-time quantitative PCR. Methods. 2001; 25:383–385. [PubMed: 11846607]

Sevcik MA, Jonas BM, Lindsay TH, Halvorson KG, Ghilardi JR, Kuskowski MA, Mukherjee P, Maggio JE, Mantyh PW. Endogenous opioids inhibit early-stage pancreatic pain in a mouse model of pancreatic cancer. Gastroenterology. 2006; 131:900–910. [PubMed: 16952558]

Sharp BM, Li MD, Matta SG, McAllen K, Shahabi NA. Expression of delta opioid receptors and transcripts by splenic T cells. Ann N Y Acad Sci. 2000; 917:764–770. [PubMed: 11268405]

Sibinga NE, Goldstein A. Opioid peptides and opioid receptors in cells of the immune system. Annu Rev Immunol. 1988; 6:219–249. [PubMed: 2838048]

Simon EJ, Hiller JM, Edelman I. Stereospecific binding of the potent narcotic analgesic (3H) Etorphine to rat-brain homogenate. Proc Natl Acad Sci USA. 1973; 70:1947–1949. [PubMed: 4516196]

Singhal PC, Abramovici M, Bansal M, Jaffer S, Mattana J, Shah R, Gibbons N. Opioids modulate migration, spreading and adherence of mesangial cells. Nephron. 1994; 68:366–371. [PubMed: 7838261]

Stein C. Peripheral mechanisms of opioid analgesia. Anesth Analg. 1993; 76:182–191. [PubMed: 8380316]

Tegeder I, Meier S, Burian M, Schmidt H, Geisslinger G, Lotsch J. Peripheral opioid analgesia in experimental human pain models. Brain. 2003; 126:1092–1102. [PubMed: 12690049]

Terenius L. Stereospecific interaction between narcotic analgesics and a synaptic plasm a membrane fraction of rat cerebral cortex. Acta Pharmacol Toxicol (Copenh). 1973; 32:317–320. [PubMed: 4801733]

Tichopad A, Pfaffl MW, Didier A. Tissue-specific expression pattern of bovine prion gene: quantification using real-time RT-PCR. Mol Cell Probes. 2003; 17:5–10. [PubMed: 12628587]

Vaughan CW, Ingram SL, Connor MA, Christie MJ. How opioids inhibit GABA-mediated neurotransmission. Nature. 1997; 390:611–614. [PubMed: 9403690]

Wittert G, Hope P, Pyle D. Tissue distribution of opioid receptor gene expression in the rat. Biochem Biophys Res Commun. 1996; 218:877–881. [PubMed: 8579608]

Yamada K, Nabeshima T. Stress-induced behavioral responses and multiple opioid systems in the brain. Behav Brain Res. 1995; 67:133–145. [PubMed: 7779288]

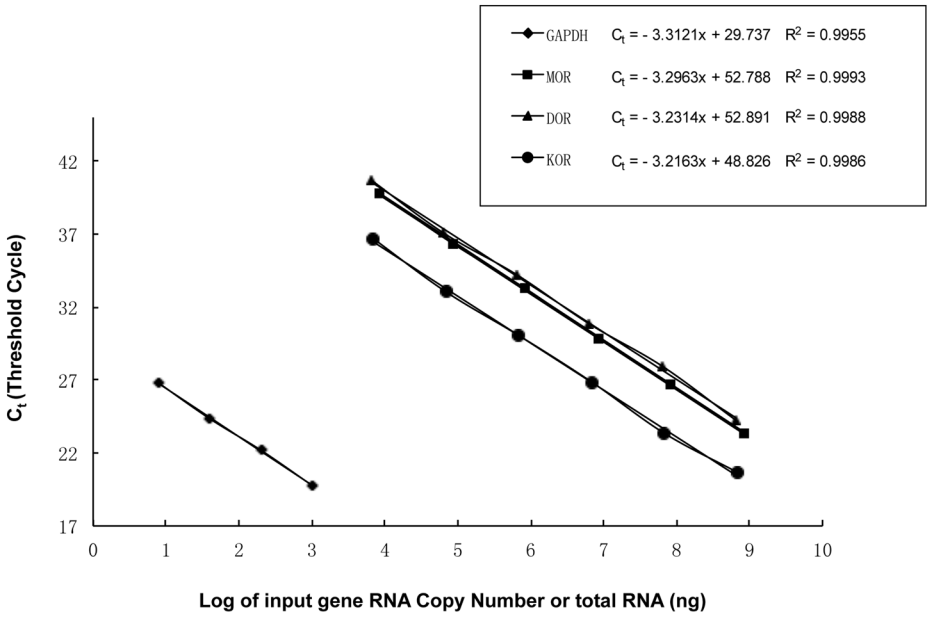

Figure 1. Standard curves for MOR, DOR, KOR, and GAPDH

Ten-fold serial dilutions of the RNA standard were amplified by real-time PCR. Threshold cycle values are plotted against input RNA copy number, or the amount of total RNA. The correlation coefficient (R2) of MOR, DOR, KOR, and GAPDH were 0.9955, 0.9993, 0.9988, and 0.9986, respectively.

Table 1

Primer sequences used in AQ-real-time RT-PCR

mRNA	Primers	Sequence (5′-3′)
MOR	Forward	TACCGTGTGCTATGGACTGAT
	Reverse	ATGATGACGTAAATGTGAATG
	Probe	CTTGCGCCTCAAGAGTGTCCGCA
DOR	Forward	GCGGGAAAGCCAGTGACTC
	Reverse	TGCCCTGTTTAAGGACTCAGTTG
	Probe	AGGAGAGGAGCGGGACCTGTGGCT
KOR	Forward	CGTCTGCTACACCCTGATGATC
	Reverse	CTCTCGGGAGCCAGAAAGG
	Probe	TGCGTCTCAAGAGCGTCCGGC
GAPDH	Forward	GGAAGCTCACTGGCATGGC
	Reverse	TAGACGGCAGGTCAGGTCCA
	Probe	CCCCACTGCCAACGTGTCAGTG

MOR: mu-OR; DOR: delta-OR; KOR: kappa-OR.

Table 2

The coefficients of variation (CV) of inter- and intra- assay threshold cycle (CT) values of the MOR, DOR, KOR, and GAPDH assay using AQ-real-time RT-PCR

Assay	Range of CV (%)			
	MOR	DOR	KOR	GAPDH
inter-	1.31 – 2.31	0.35 – 2.90	1.32 – 1.87	1.68 – 2.08
intra-	0.60 – 1.89	0.08 – 2.77	0.47 – 1.46	0.18 – 1.67

Table 3

Inter-assay reproducibility of KOR mRNA quantification using AQ-real-time RT-PCR

Assay no	C_t for no. of input copies[a]				
	68300000[b]	6830000[c]	683000[d]	68300[e]	6830[f]
	21.62	24.32	27.76	31.07	34.11
	21.76	24.47	27.81	31.01	33.63
	20.96	23.82	27.76	31.00	34.18
	21.85	24.52	28.64	32.04	34.87

[a] Input copy numbers of KOR RNA standard

[b] Mean ± standard error of the mean, 21.55 ± 0.40; CV, 1.87%

[c] Mean ± standard error of the mean, 24.28 ± 0.32; CV, 1.32%

[d] Mean ± standard error of the mean, 27.99 ± 0.43; CV, 1.54%

[e] Mean ± standard error of the mean, 31.28 ± 0.51; CV, 1.62%

[f] Mean ± standard error of the mean, 34.20 ± 0.51; CV, 1.49%

Table 4

Intra-assay accuracy of AQ-real-time RT-PCR for quantification of KOR mRNA in human tissues

Repetition no.	C_t for KOR mRNA in:							
	SN[a]	CC[b]	TL[c]	Pu[d]	Lu[e]	FB[f]	AG[g]	ST[h]
1	29.96	27.81	28.43	26.51	33.76	26.25	34.92	34.79
2	29.16	28.35	28.32	29.69	34.13	26.29	34.82	34.85
3	28.89	28.02	28.21	26.53	33.83	25.82	34.81	34.00
4	29.27	28.13	28.51	26.48	33.71	25.93	34.45	34.00
5	28.88	28.29	28.16	26.81	34.32	26.15	34.95	34.03
6	28.84	28.01	28.38	26.98	34.00	26.20	35.37	34.11

SN, *substantia nigra*; CC, *cerebral cortex*; TL, *temporal lobe*; Pu, *putamen*, Lu, *Lung*; FB, *fetal – brain*; AG, *adrenal gland*; SI, *small intestine*

[a] Mean ± standard error of the mean, 29.17 ± 0.43; CV, 1.46%

[b] Mean ± standard error of the mean, 28.10 ± 0.71; CV, 0.71%

[c] Mean ± standard error of the mean, 28.34 ± 0.13; CV, 0.47%

[d] Mean ± standard error of the mean, 26.67 ± 0.20; CV, 0.70%

[e] Mean ± standard error of the mean, 33.96 ± 0.24; CV, 0.70%

[f] Mean ± standard error of the mean, 26.11 ± 0.19; CV, 0.72%

[g] Mean ± standard error of the mean, 34.87 ± 0.27; CV, 0.76%

[h] Mean ± standard error of the mean, 34.30 ± 0.41; CV, 1.20%

Table 5

AQ-real-time RT-PCR of MOR, DOR, and KOR mRNA in 22 human tissues

Tissue	MOR (mean (S.D.))	DOR (mean (S.D.))	KOR (mean (S.D.))
Lung	---	46,691 (11683)	41,689 (10865)
Spleen	---	---	69,169 (6639)
Kidney	---	19,996 (3022)	449 (195)
Heart	---	3,810 (343)	6,363 (477)
Skeletal Muscle	---	636,289 (113975)	633 (53)
Liver	---	---	22,956 (1046)
Thymus	---	58,634 (9911)	82,663 (10087)
Small Intestine	193,566 (30949)	297,430 (7037)	19,819 (9911)
Pancreas	202,079 (52357)	1,897,559 (610848)	5,562 (125)
Adrenal Gland	3,627,481 (53101)	2,486,048 (348827)	18,743 (3314)
Dorsal Root Ganglion	6, 151,528 (2627627)	8, 845,040 (1167770)	1, 220,028 (99402)
Spinal Cord	5,002,216 (1120700)	627,411 (164391)	153,391 (5690)
Fetal Brain	2,655,362 (395172)	7,541,072 (2478317)	3,810,443 (454190)
Brain	5,483,142 (304908)	15,829,475 (937822)	500,625 (17911)
Substantia Nigra	2,422,351 (234406)	1,511,108 (444127)	1,200,376 (153403)
Hippocampus	2,691,485 (600971)	15,995,085 (1963678)	1,239,650 (237016)
Temporal Lobe	2,705,526 (349830)	19,726,728 (8028636)	643,648 (52430)
Cerebral Cortex	6,438,479 (1741192)	22,559,696 (825512)	1,365,055 (221019)
Putamen	8,184,267 (531979)	20,436,532 (7029328)	4,253,240 (132830)
Caudate Nucleus	12,784,025 (1388657)	21,252,144 (284668)	2,698,974 (378423)
Nucleus Accumbens	17,197,758 (3290975)	21,624,589 (2733506)	3,982,715 (133555)
Cerebellum	19,215,581 (173929)	268,123 (17369)	531,658 (29013)

Data are given as copies/μg of RNA